Electrical insulation properties of the perfluoronitrile C4F7N

Author(s):
Chachereau, Alise; Hösl, Andreas; Franck, Christian

Publication date:
2018-12-12

Permanent link:
https://doi.org/10.3929/ethz-b-000262561

Originally published in:
Journal of Physics D: Applied Physics 51(49), https://doi.org/10.1088/1361-6463/aae458

Electrical insulation properties of the perfluoronitrile C_4F_7N

A. Chachereau[1], **A. Hösl**[1], **C. M. Franck**[1]

[1]Power Systems and High Voltage Laboratories, ETH Zurich, Physikstr. 3, 8092 Zurich, Switzerland

E-mail: alisec@ethz.ch

Abstract. The electrical insulation properties of pure C_4F_7N and of C_4F_7N/N_2 and C_4F_7N/CO_2 mixtures are investigated in a pulsed Townsend setup. The electron rate and transport coefficients and the density-reduced critical electric field of these mixtures are obtained, and a synergy effect is observed in C_4F_7N/N_2 and C_4F_7N/CO_2 mixtures. The total electron attachment cross section of C_4F_7N is estimated based on the attachment rate to C_4F_7N in diluted C_4F_7N/N_2, C_4F_7N/CO_2 and $C_4F_7N/O_2/CO_2$ mixtures. Measurements in pure C_4F_7N at pressures of a few hundred pascal show that ion kinetics play a major role in C_4F_7N discharges and that further modelling is required to assess the electric strength of C_4F_7N at high pressures.

Introduction

The perfluorinated nitrile $(CF_3)_2CFC{\equiv}N$, which we refer to in the following as C_4F_7N, has been proposed as an environment-friendly alternative to SF_6 in high voltage gaseous electrical insulation [1, 2]. The first pilot installations using this gas are a 420 kV gas insulated line in Sellinge, UK [3] and a 145 kV gas insulated substation in Etzel, Switzerland. The manufacturer reports a low toxicity and recommends an occupational exposure limit of 65 ppm for C_4F_7N [4]. Different estimations place the GWP of C_4F_7N on a 100 year time horizon between 1490 and 3646, with an atmospheric lifetime between 22 and 47 years [4, 5, 6]. The main removal mechanism of C_4F_7N from the atmosphere is reactions with hydroxyl radicals [4, 5, 6]. Due to the limited vapor pressure of C_4F_7N, mixtures of 4 to 10% C_4F_7N in CO_2 (in some cases, up to 10% CO_2 is replaced by O_2) are used in electrical insulation with minimum operating temperatures of down to -25°C [7]. The GWP of these mixtures range from 230 to 1240, which is a significant reduction compared to the GWP of SF_6 of 23 500 [8].

In this work, we investigate both C_4F_7N/CO_2 and C_4F_7N/N_2 mixtures in a pulsed Townsend setup. We start with the description of the experimental setup, the experimental conditions and the measurement analysis. In the second part of this work, we present measurement results in diluted mixtures of C_4F_7N in N_2, in CO_2 and in a $95\%O_2/5\%CO_2$ mixture, and use these to estimate the electron attachment cross section of C_4F_7N. In pure C_4F_7N at pressures of several hundred pascal, we show that the measured current is largely influenced by ion kinetic processes. Therefore, we restrict ourselves to low pressures and present the rate coefficients of ionization, attachment, and effective ionization, as well as the electron drift velocity and the longitudinal electron diffusion coefficient. Furthermore, we measure the properties of C_4F_7N/CO_2 and C_4F_7N/N_2 mixtures with C_4F_7N percentages up to 40%, in order to investigate the synergism of the density-reduced critical electric field. We compare these results to those in C_4F_7N/CO_2 mixtures recently obtained by Nechmi et al. using a steady-state Townsend experiment [9]. We make all our data available on the database ETHZ [10] from the LXcat project.

1. Methods

1.1. Swarm experiment

The experiment consists in measuring the electric displacement current of electrons and ions in different gas mixtures, for different ratios of the electric field to the gas density E/N. The gas, or gas mixture under test is filled into a stainless steel vessel containing two Rogowski electrodes with adjustable spacing d, across which a voltage U is applied. A photocathode, i.e. a quartz covered with a double-layer of 15 nm magnesium and 5 nm palladium, is mounted at the center of the cathode. A UV-laser pulse with a wavelength of 266 nm and a pulse duration of 1.5 ns FWHM releases 10^6 to 10^7 electrons from the photocathode. Due to the applied electric field, the released electrons drift towards the anode and initiate an electron avalanche. Electrons colliding with gas molecules may ionize them, forming positive ions and releasing new electrons, or may be captured, forming negative ions. Ions drift as well, contributing, relative to their drift velocity, to the measured displacement current. For the present measurements, the laser power was regulated down in order to keep a total charge below 5×10^{-12} C.

1.1.1. Experimental setup The measurements in the diluted C_4F_7N/N_2, C_4F_7N/CO_2 and $C_4F_7N/O_2/CO_2$ mixtures presented in section 2.1 were performed

in the pulsed Townsend setup that was described in [11], whereas the subsequent measurements with higher C_4F_7N percentages were performed in a newly available setup [12] which allows for more accurate electrode spacing ($\pm 10\,\mu m$ instead of $\pm 100\,\mu m$), leading to a higher accuracy in E/N.

1.1.2. Gas purity The vessel has a base pressure of 1×10^{-6} Pa. In order to fill a gas or gas mixture, the content of the inlet pipes is first evacuated through the vessel. Then, each of the inlet pipes is flushed with one of the gases under study. Finally, the vessel is evacuated again and closed. The residual pressure in the vessel before the gas is filled is below 0.1 Pa. The gases used in the present work are C_4F_7N with a purity of at least 99 mole % (3M), N_2 with a purity of 6.0 (Carbagas), and CO_2 with a purity of 4.8 (Carbagas).

1.2. Measurement analysis

The measured current I_{exp} is the superposition of the electron and ion currents. These two components are separated using an iterative procedure [13] and analyzed as follows.

1.2.1. Electron current analysis The electron current analysis was described in detail in a previous publication [13]. Assuming that the one-dimensional electron density along the avalanche propagation axis is Gaussian, the electron current I_e is expressed analytically for $t \geq 0$ as [11, 13]

$$I_e(t) = \frac{I_0}{2} e^{k_{eff} N t} \left(1 - \mathrm{erf}\left(\frac{t - T_e}{\sqrt{2\tau_D t}}\right)\right), \tag{1}$$

$$I_0 = \frac{N_e(0) q_0}{T_e}, \tag{2}$$

where I_0 is the electron current at time $t = 0$, k_{eff} is the effective ionization rate coefficient, N is the number density of the gas, T_e is the electron drift time, which relates to the bulk electron drift velocity w_e via $T_e = d/w_e$, τ_D is the characteristic time for longitudinal electron diffusion, which relates to the longitudinal diffusion coefficient D_L via $2D_L = w_e^2 \tau_D$, $N_e(0)$ is the number of electrons released from the photocathode and q_0 is the elementary charge.

1.2.2. Ionization and attachment rates Using the integral of the measured current I_{exp} as described in [14], the ionization and attachment rate coefficients k_i and k_a are obtained as

$$k_i = k_{eff} \frac{N_{charges}^{final} - N_e(0)}{N_e(T_e) - N_e(0)}, \tag{3}$$

$$k_a = k_i - k_{eff} = k_{eff} \frac{N_{charges}^{final} - N_e(T_e)}{N_e(T_e) - N_e(0)}. \tag{4}$$

where $N_{charges}^{final}$ is the final number of electrons at the instant when they reach the anode, and $N_{charges}^{final}$ is the total number of charges in the avalanche

$$N_{charges}^{final} = \frac{1}{q_0} \int_0^\infty I_{exp}(t) \mathrm{d}t. \tag{5}$$

As mentioned in [14], this method relies on the assumption that no ionization events occur after the electron drift time T_e, for instance due to electron detachment from negative ions, since this would increase the measured current and result in overestimating the values of k_i and k_a. In the limit of low pressures this assumption is justified because the ion-neutral collisions become negligible.

1.2.3. Estimating the total electron attachment cross section The total attachment cross section of C_4F_7N is estimated by two methods [15], using the effective ionization coefficient measured in diluted mixtures of C_4F_7N in N_2, in CO_2 and in the mixture of 95% O_2/5% CO_2, under the assumption that the C_4F_7N admixture does not disturb the electron energy distribution function of the carrier gas (i.e. N_2, CO_2 or 95% O_2/5% CO_2). In this case, the relation between the attachment cross section of C_4F_7N σ_a and the measured values of k_{eff} in the C_4F_7N mixtures is

$$k_{eff}^{[mixture]} = (1 - x) k_{eff}^{[carrier\ gas]} + x \sqrt{\frac{2}{m_e}} \int_0^\infty (\sigma_i - \sigma_a) \varepsilon f^{[carrier\ gas]} \mathrm{d}\varepsilon, \tag{6}$$

where x is the mole fraction of C_4F_7N in the mixture, m_e is the electron mass, σ_i is the ionization cross section of C_4F_7N and $f^{[carrier\ gas]}$ is the electron energy distribution function in the carrier gas. At the considered low mole fractions of C_4F_7N and low E/N values, the contribution of the ionization cross section σ_i of C_4F_7N is negligible. This was verified using the calculated ionization cross section of C_4F_7N by Xiong et al. [16].

The first method to obtain the attachment cross section of C_4F_7N is a linear inversion method, which makes no assumption on the shape of the cross section and requires no initial guess of the solution. We denote by $\sigma_a^{(li)}$ the cross section obtained by this method. The second method is a Gaussian expansion, i.e. the shape of the cross section is approximated by the sum of several Gaussian functions. Likewise, we denote by $\sigma_a^{(ge)}$ the cross section obtained by this method. We find in section 2.2 that in the present case, the cross section is well fitted with two terms, i.e.

$$\sigma_a^{(ge)}(\varepsilon) = \sum_{i=1}^{2} c_i e^{-(\varepsilon - \varepsilon_i)^2/(2s_i^2)}, \tag{7}$$

where c_i, ε_i and s_i are the amplitude, position and width of the Gaussian peaks, determined by the fit.

Table 1. Overview of the measurements in the diluted C_4F_7N/N_2 and C_4F_7N/CO_2 mixtures.

buffer gas	C_4F_7N mol%	(E/N)-range (Td)	pressures (kPa)
N_2	0	5 - 180	2, 10
	0.010	2 - 120	10
	0.050	15 - 145	8, 10
	0.125	50 - 160	8, 10
CO_2	0	5 - 140	2, 10
	0.010	6 - 95	2, 10
	0.022	10 - 100	10
	0.044	25 - 103	8, 10
95% O_2- 5% CO_2	0	1 - 100	1
	0.090	1 - 100	1

Both methods require the knowledge of the electron energy distribution function (EEDF) in the carrier gases. In the present work the EEDF in N_2, CO_2 and in the mixture of 95% O_2/5% CO_2 is obtained using the solver Bolsig+ [17], with Biagi's cross section sets for N_2 and O_2 [18] and Phelps' cross section set for CO_2 [19]. The effective ionization rate coefficient, electron drift velocity and diffusion coefficients calculated in pure N_2, in pure CO_2 and in the mixture of 95% O_2/5% CO_2 are shown in figures 1, 2 and 3 respectively.

In order to verify the assumption of an undisturbed EEDF, additional Bolsig+ simulations were carried out in the C_4F_7N mixtures under study. The above-mentioned cross section sets were used for the carrier gases, and for C_4F_7N only the attachment cross section $\sigma_a^{(ge)}$ obtained in the present work was considered. In the investigated E/N range, no significant difference was observed between the EEDFs of the C_4F_7N mixtures under study and the EEDFs of the pure carrier gases.

2. Results

2.1. Diluted C_4F_7N/N_2 and C_4F_7N/CO_2 mixtures

An overview of the measurements in diluted mixtures of C_4F_7N with N_2 and CO_2 is given in table 1. The obtained effective ionization rate coefficient, electron drift velocity and diffusion coefficient are shown in figure 1 for N_2 mixtures and figure 2 for CO_2 mixtures. The effective ionization coefficient in diluted C_4F_7N mixtures is decreasing with increasing C_4F_7N content due to electron attachment to C_4F_7N.

2.2. Electron attachment cross section

Using the values of k_{eff} obtained in the diluted C_4F_7N/N_2 and C_4F_7N/CO_2 mixtures, the total attachment cross section of C_4F_7N is estimated with

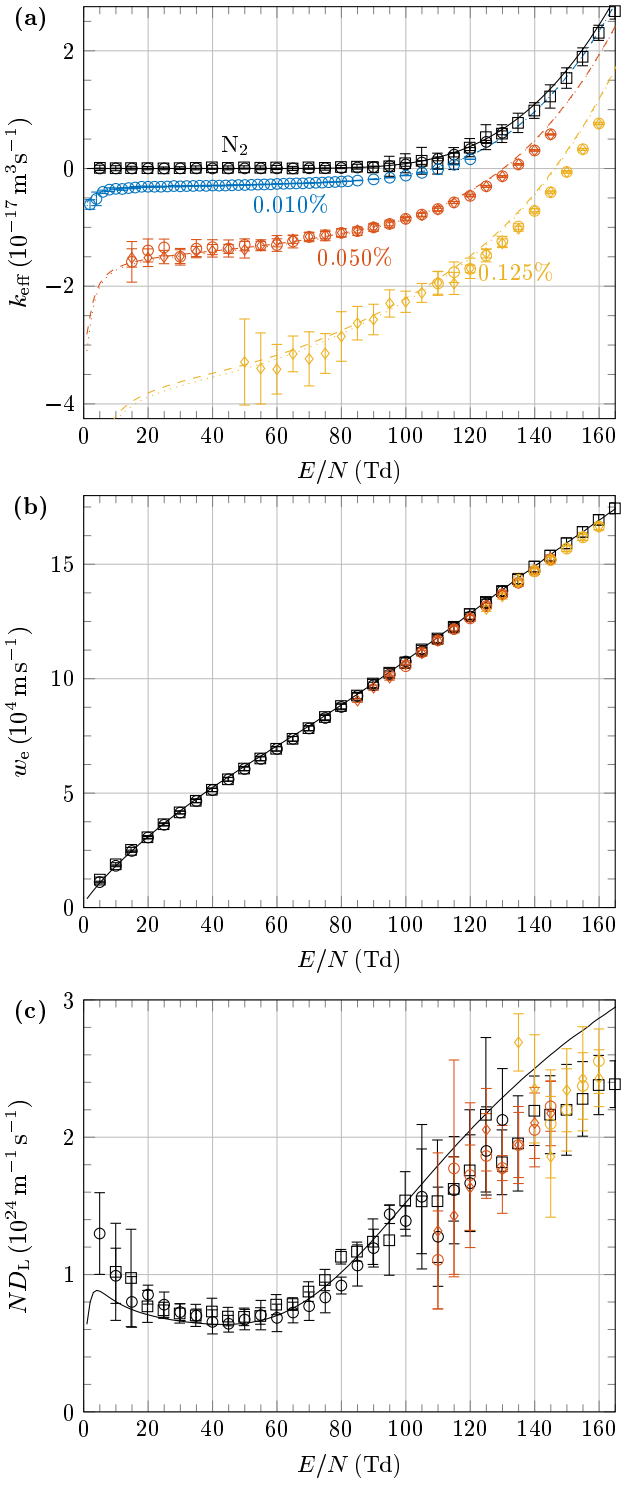

Figure 1. **(a)** Effective ionization rate coefficient, **(b)** electron drift velocity and **(c)** electron diffusion coefficient as functions of E/N in C_4F_7N/N_2 mixtures. The gas mixtures are color-coded, the C_4F_7N percentages are indicated in figure (a). The gas pressures are indicated with different marker shapes (□ 2 kPa, ◇ 8 kPa, ○ 10 kPa). The lines correspond to:
—— k_{eff}, w_e and ND_L in N_2, calculated using Bolsig+
- - - k_{eff} in C_4F_7N/N_2 mixtures, calculated using $\sigma_a^{(li)}$
····· k_{eff} in C_4F_7N/N_2 mixtures, calculated using $\sigma_a^{(ge)}$

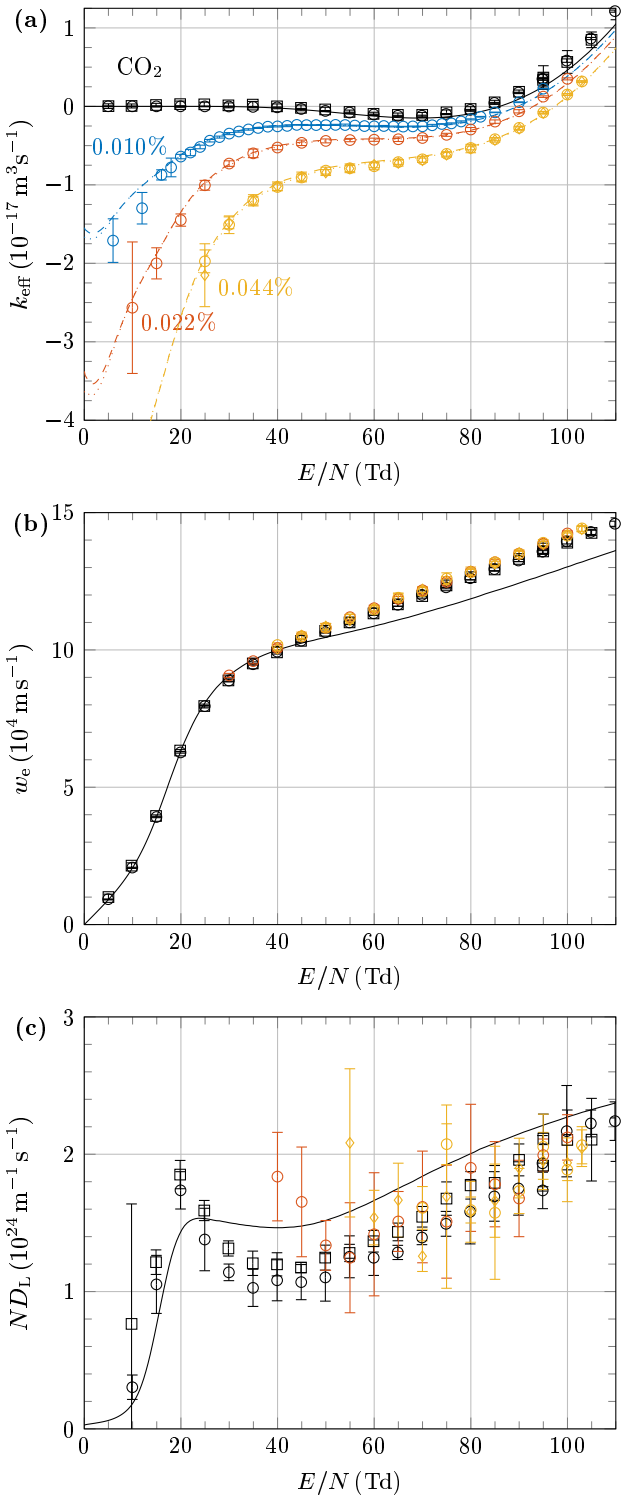

Figure 2. **(a)** Effective ionization rate coefficient, **(b)** drift velocity and **(c)** diffusion coefficient as functions of E/N in C_4F_7N/CO_2 mixtures. The gas mixtures are color-coded, the C_4F_7N percentages are indicated in figure (a). The gas pressures are indicated with different marker shapes (□ 2 kPa, ◇ 8 kPa, ○ 10 kPa). The lines correspond to:
—— k_{eff}, w_e and ND_L in CO_2, calculated using Bolsig+
- - - k_{eff} in C_4F_7N/CO_2 mixtures, calculated using $\sigma_a^{(li)}$
····· k_{eff} in C_4F_7N/CO_2 mixtures, calculated using $\sigma_a^{(ge)}$

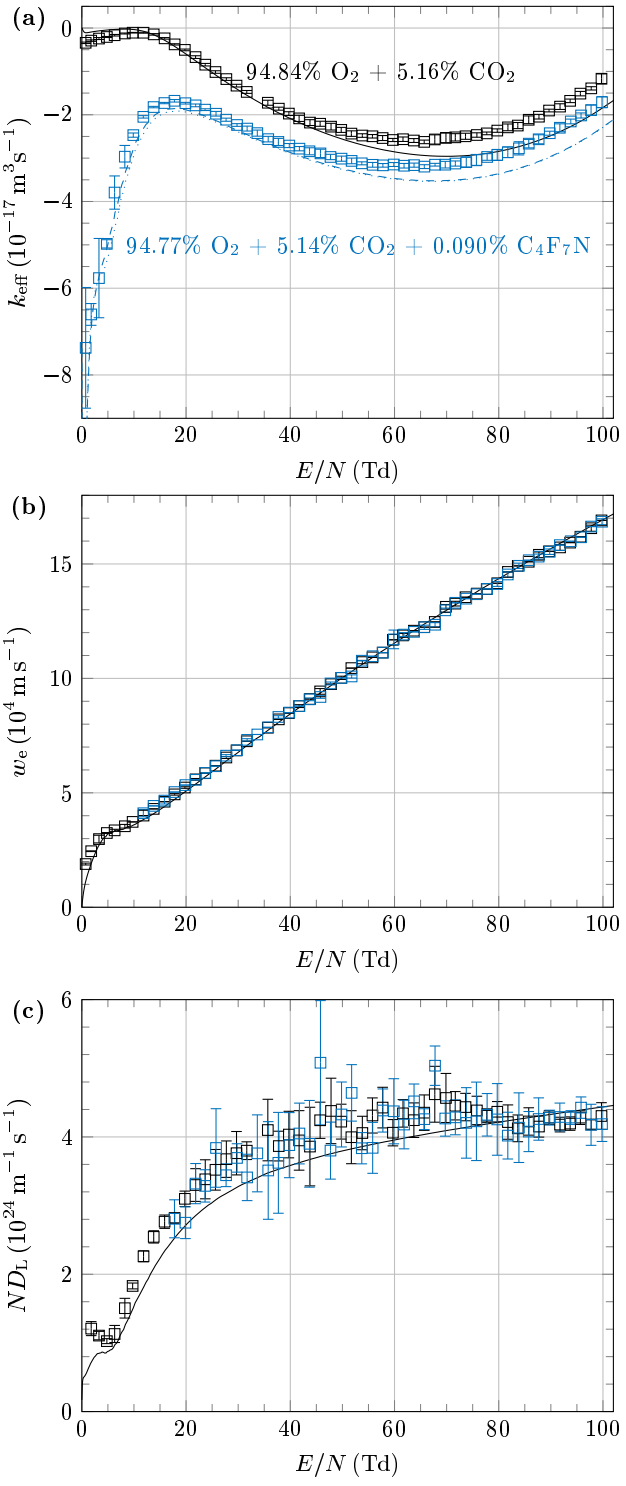

Figure 3. **(a)** Effective ionization rate coefficient, **(b)** drift velocity and **(c)** diffusion coefficient as functions of E/N in the mixture of 5.16% CO_2 in O_2 and in the mixture of 0.090% C_4F_7N and 5.14% CO_2 in O_2, at a total pressure of 1 kPa. The gas mixtures are color-coded as indicated in figure (a). The lines correspond to:
—— k_{eff}, w_e and ND_L in the O_2/CO_2 mixture, Bolsig+
- - - k_{eff} in the $C_4F_7N/O_2/CO_2$ mixture, calculated using $\sigma_a^{(li)}$
····· k_{eff} in the $C_4F_7N/O_2/CO_2$ mixture, calculated using $\sigma_a^{(ge)}$

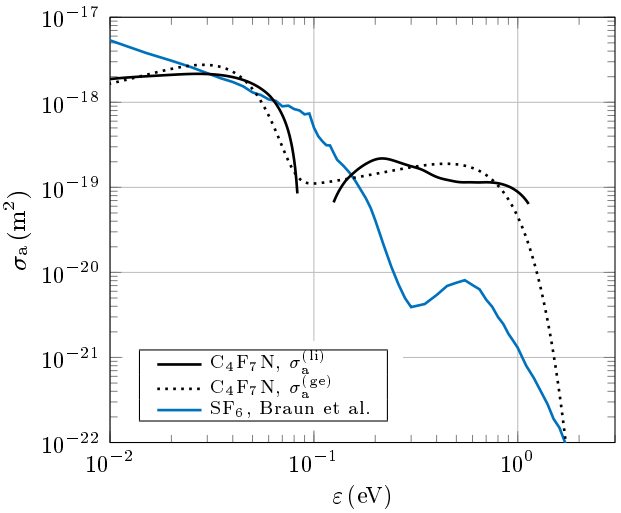

Figure 4. Total attachment cross section of SF_6 and estimated total electron attachment cross section of C_4F_7N.

the linear inversion and the Gaussian expansion methods as described in section 1.2.3. The resulting cross sections $\sigma_a^{(li)}$ and $\sigma_a^{(ge)}$ are shown in figure 4, along with the electron attachment cross section of SF_6 measured by Braun et al. [20]. Below 0.1 eV $\sigma_a^{(li)}$ and $\sigma_a^{(ge)}$ are in good agreement and have about the same magnitude as the cross section of SF_6. Above 0.1 eV, $\sigma_a^{(li)}$ and $\sigma_a^{(ge)}$ are larger than the attachment cross section of SF_6, and sustained up to 1 eV. The effective ionization rate coefficient in the diluted C_4F_7N/N_2 and C_4F_7N/CO_2 mixtures, was calculated using the cross sections $\sigma_a^{(li)}$ and $\sigma_a^{(ge)}$ to check the quality of the estimations. The calculated values of k_{eff}, shown in figures 1(a) and 2(a), fit perfectly with the measured values and each other over the whole E/N range. It can be seen that despite the differences between $\sigma_a^{(li)}$ and $\sigma_a^{(ge)}$, both are resolved to a maximal extent based on the present measurements. For the same reason, it is not reasonable to add a third term to the Gaussian expansion $\sigma_a^{(ge)}$, as the two term expansion already fits perfectly the measurements.

2.3. Results in pure C_4F_7N

Example measurements carried out in pure C_4F_7N at pressures up to 1 kPa are shown in figure 5. The measured current at 1 kPa features a maximum at $t \sim 10\,\mu s$, i.e. on the ionic timescale, which suggests that ion kinetics play a major role in high pressure C_4F_7N discharges. Furthermore, when using equations (3) and (4) with measurements in C_4F_7N at 260 to 1000 Pa, the obtained values for k_i and k_a increase with increasing gas pressure. These inconsistent values for k_i and k_a suggest that ionization events occur

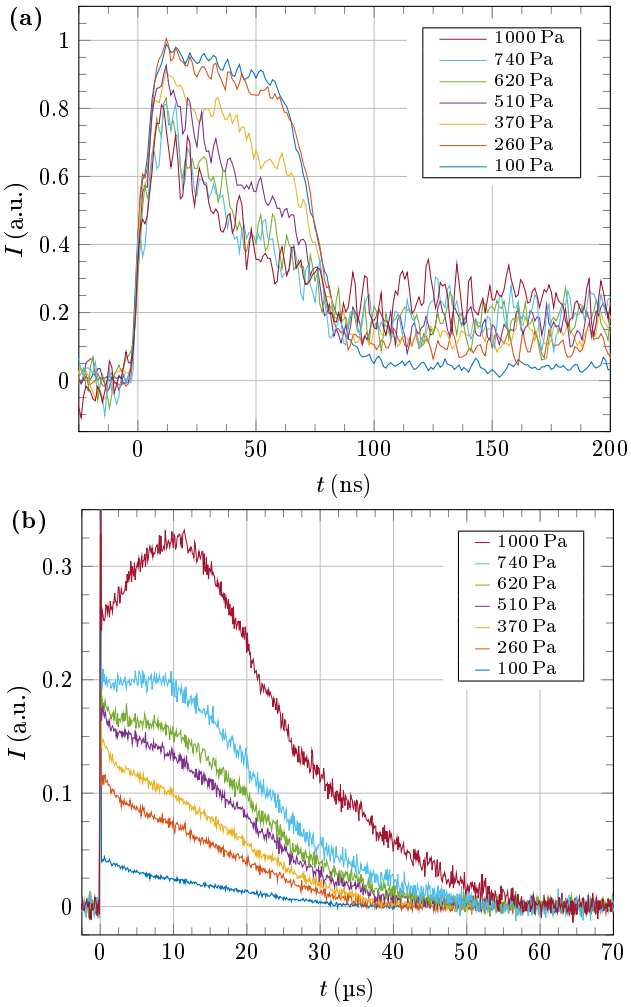

Figure 5. Current versus time in pure C_4F_7N, at different pressures, for an electrode spacing of 25 mm, and for a reduced electric field E/N of 966 Td, **(a)** on the electronic timescale and **(b)** on the ionic timescale. The measurements are rescaled to have a similar amplitude at $t = 0$, the original amplitudes ranged from 5.5 µA at 100 Pa to 0.4 µA at 1000 Pa.

after the electron drift time T_e, for instance due to electron detachment from negative ions. When the kinetic model is known, it is possible to obtain the rate coefficients for both electron and ion processes by fitting the measured current, as this was done first for humid air [21], and more recently for N_2-O_2 mixtures [22, 23]. However, no information is yet available as to which negative ions are formed in C_4F_7N, and which of those might be prone to electron detachment. Therefore, the analysis of high pressure measurements in C_4F_7N will require first an extensive modelling of the ion kinetics. In the meantime, we restrict ourselves to low pressures where the ion kinetics are negligible. We report electron rate and transport coefficients in pure C_4F_7N for pressures ranging from 60 to 100 Pa. Example measurements in C_4F_7N at 100 Pa are shown in figures 6 and 7.

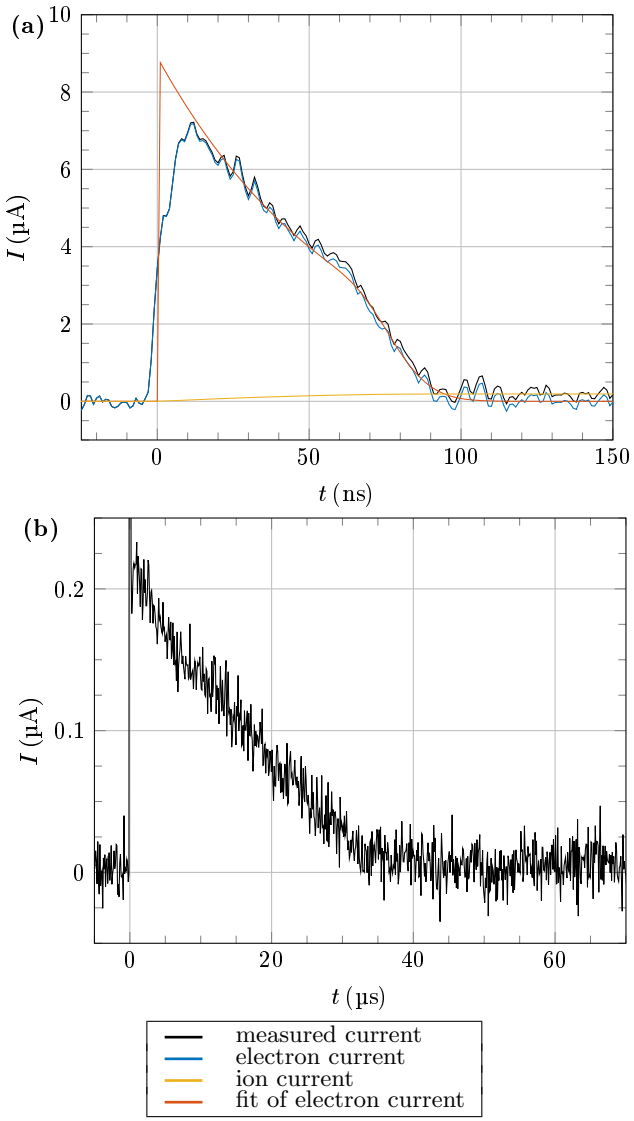

Figure 6. Current versus time in pure C_4F_7N, at a pressure of 100 Pa, for an electrode spacing of 25 mm, and for a reduced electric field E/N of 916 Td **(a)** on the electronic timescale and **(b)** on the ionic timescale.

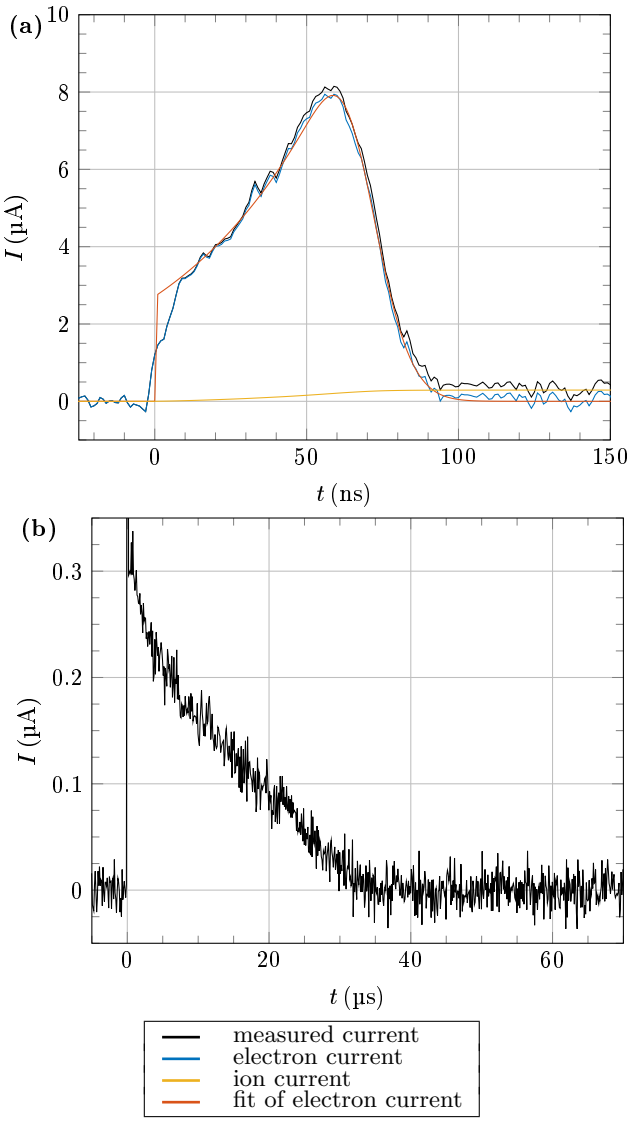

Figure 7. Current versus time in pure C_4F_7N, at a pressure of 100 Pa, for an electrode spacing of 25 mm, and for a reduced electric field E/N of 1047 Td **(a)** on the electronic timescale and **(b)** on the ionic timescale.

Figure 8 shows the ionization, attachment and effective ionization rate coefficients, as well as the electron drift velocity and diffusion coefficient obtained in pure C_4F_7N at low pressures. All these quantities are independent of the gas pressure. In particular, the fact that the obtained values of the k_i and k_a are independent of the gas pressure in the considered range of 60 to 100 Pa allows us to verify that electron detachment is indeed negligible at these pressures. We obtain a density-reduced critical electric field $(E/N)_{crit}$ of 975 ± 15 Td for pure C_4F_7N. Since we consider here low pressures at which the ion kinetics of C_4F_7N are negligible, the effective ionization coefficient is defined simply as $k_{eff} = k_i - k_a$ and the density-reduced critical electric field is defined in the classical sense as the E/N ratio for which $k_i = k_a$. However, at higher pressures, ion kinetics will lead to different values of k_{eff}, and self-sustained discharges will occur at $E/N < (E/N)_{crit}$. Therefore, the present values of $(E/N)_{crit}$ are not directly usable at high pressures. A complete kinetic model will need to be developed for C_4F_7N, and the reaction rate coefficients of ionic reactions will need to be determined. Once this is achieved, it will open the way for calculations to predict the discharge development in C_4F_7N at high pressures, as it was done for humid air [21], N_2-O_2 mixtures [22, 23, 24] and CO_2 [25].

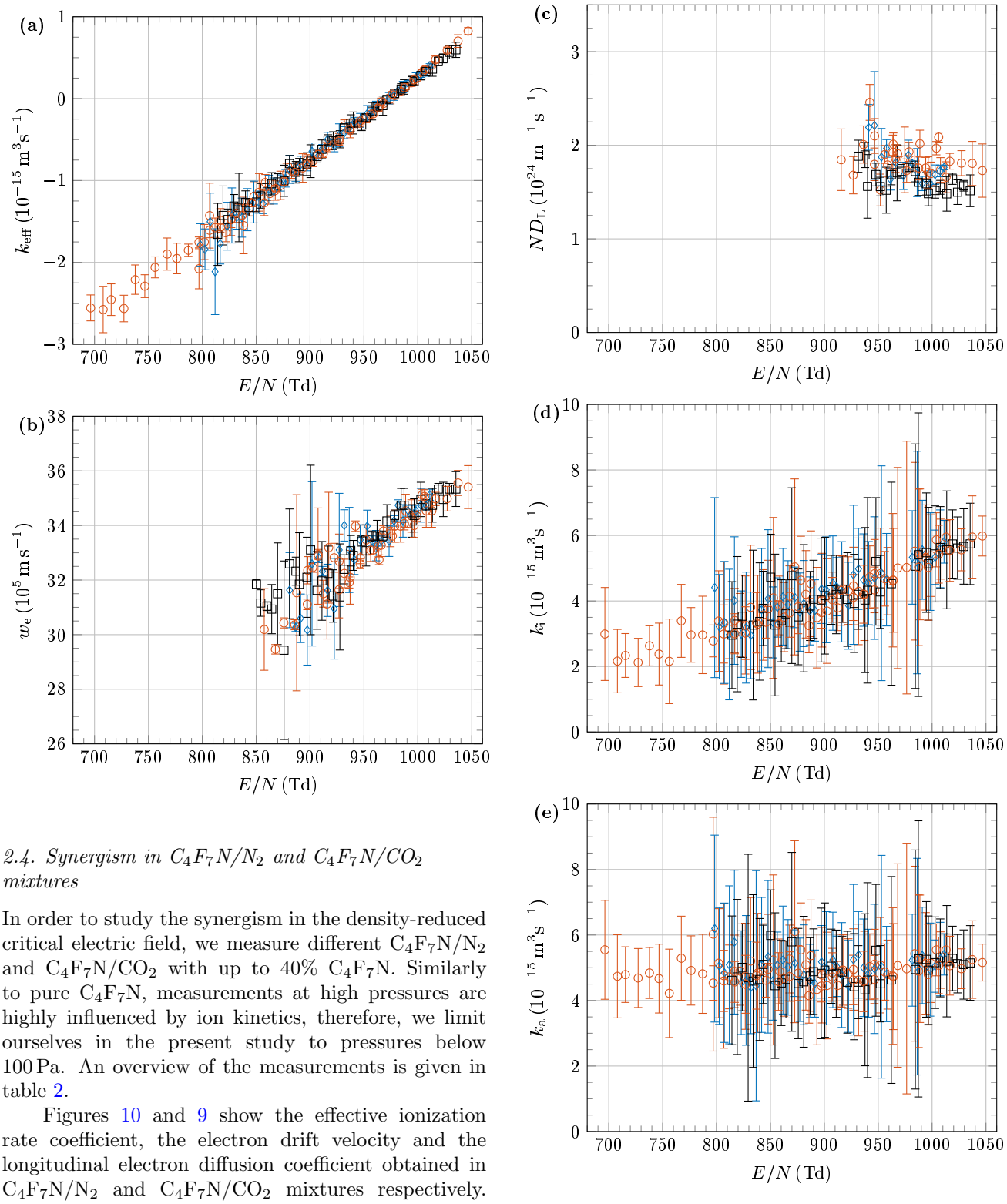

Figure 8. **(a)** Effective ionization rate coefficient, **(b)** electron drift velocity, **(c)** electron diffusion coefficient, **(d)** ionization rate coefficient and **(e)** attachment rate coefficient as functions of E/N in C_4F_7N, at different gas pressures (□ 60 Pa, ◇ 80 Pa, ○ 100 Pa).

2.4. Synergism in C_4F_7N/N_2 and C_4F_7N/CO_2 mixtures

In order to study the synergism in the density-reduced critical electric field, we measure different C_4F_7N/N_2 and C_4F_7N/CO_2 with up to 40% C_4F_7N. Similarly to pure C_4F_7N, measurements at high pressures are highly influenced by ion kinetics, therefore, we limit ourselves in the present study to pressures below 100 Pa. An overview of the measurements is given in table 2.

Figures 10 and 9 show the effective ionization rate coefficient, the electron drift velocity and the longitudinal electron diffusion coefficient obtained in C_4F_7N/N_2 and C_4F_7N/CO_2 mixtures respectively. For the C_4F_7N/CO_2 mixtures, only part of the measurements from table 2 are shown in figure 9, the rest are available on the LXcat database ETHZ [10].

The density-reduced critical electric field $(E/N)_{\mathrm{crit}}$ of C_4F_7N/N_2 and C_4F_7N/CO_2 mixtures obtained in the present work is shown in figure 11 and compared to that of C_4F_7N/CO_2 mixtures from Nechmi

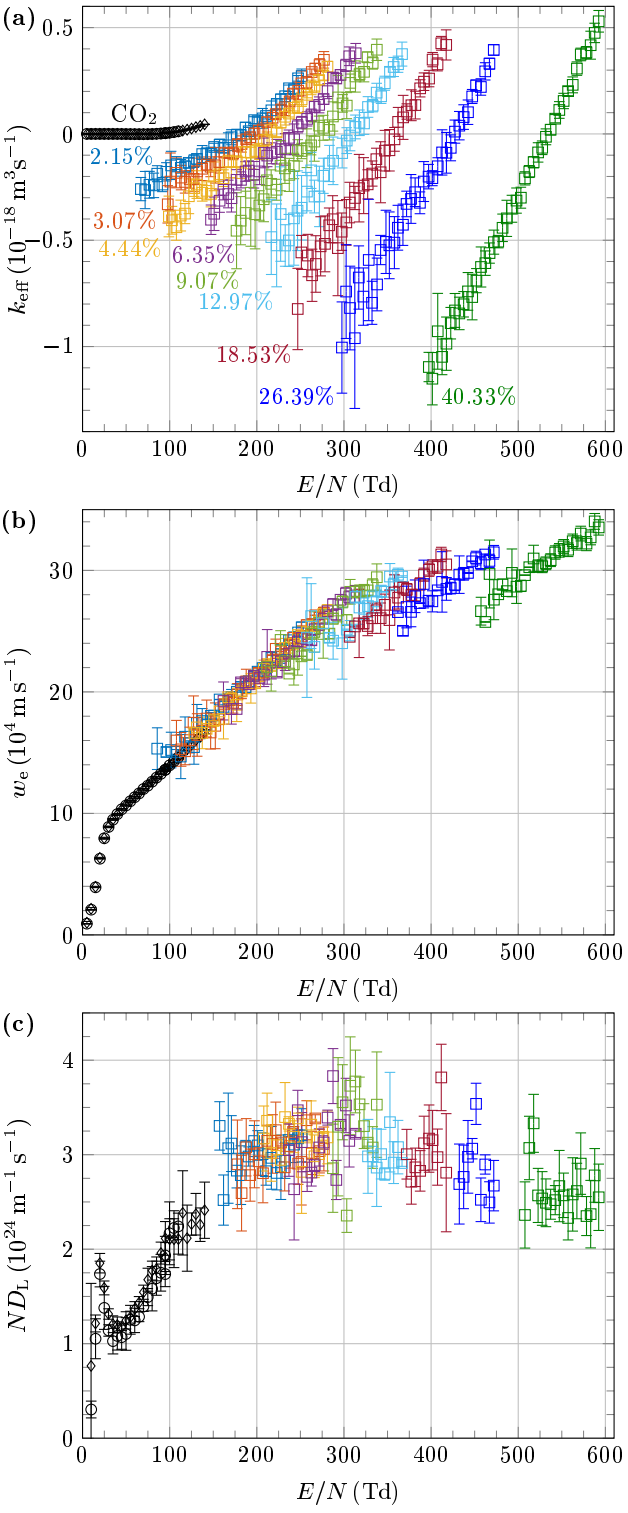

Figure 9. **(a)** Effective ionization rate coefficient, **(b)** electron drift velocity and **(c)** electron diffusion coefficient as functions of E/N in C_4F_7N/CO_2 mixtures. The gas mixtures are color-coded, the C_4F_7N percentages are indicated in figure (a). The gas pressures are indicated with different marker shapes (□ 100 Pa, ⋄ 2 kPa, ○ 10 kPa).

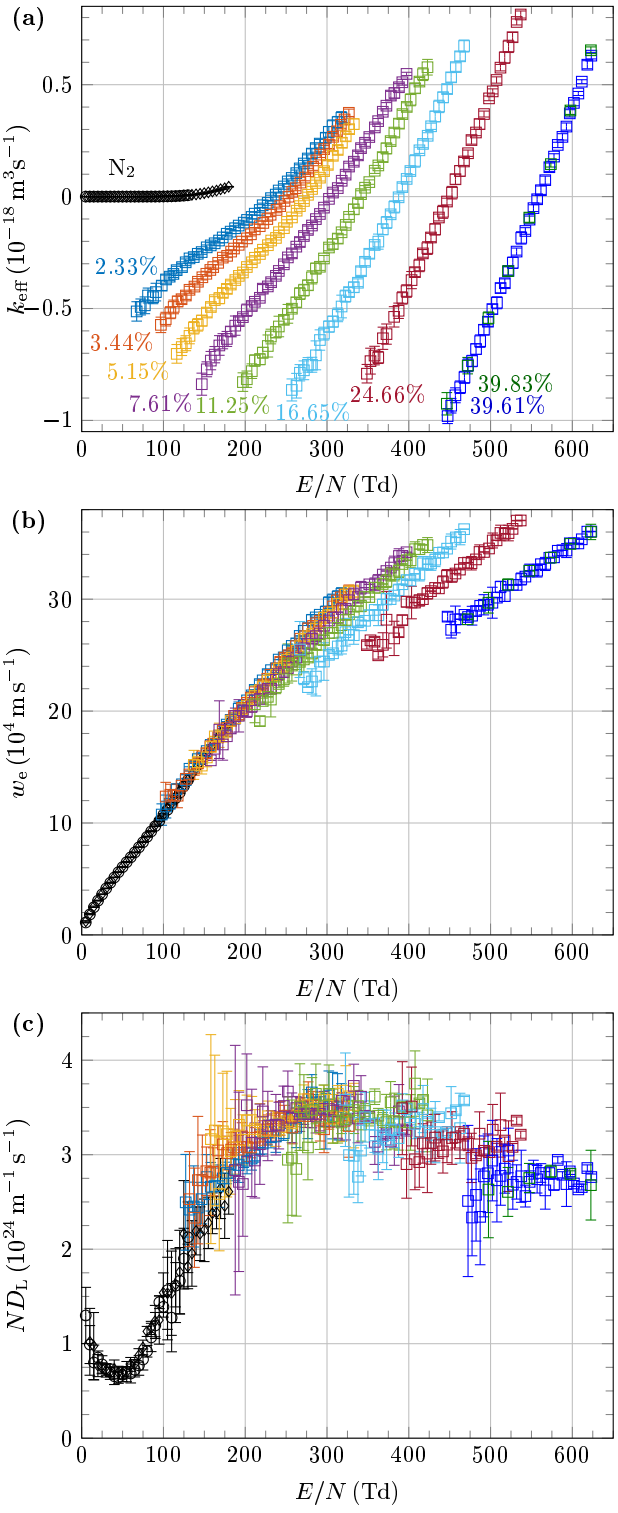

Figure 10. **(a)** Effective ionization rate coefficient, **(b)** electron drift velocity and **(c)** electron diffusion coefficient as functions of E/N in C_4F_7N/N_2 mixtures. The gas mixtures are color-coded, the C_4F_7N percentages are indicated in figure (a). The gas pressures are indicated with different marker shapes (□ 100 Pa, ⋄ 2 kPa, ○ 10 kPa).

Table 2. Overview of the measurements in the C_4F_7N/N_2 and C_4F_7N/CO_2 mixtures.

buffer gas	C_4F_7N mol%	(E/N)-range (Td)	pressures (Pa)
N_2	0	5 - 180	2000, 10000
	2.33	67 - 318	100
	3.44	97 - 327	100
	5.15	116 - 333	100
	7.61	147 - 397	100
	11.25	197 - 423	100
	16.65	257 - 468	100
	24.66	349 - 537	100
	39.61	447 - 623	100
	39.83	447 - 623	100
CO_2	0	5 - 140	2000, 10000
	2.15	67 - 251	100
	3.07	98 - 277	100
	4.44	99 - 281	100
	6.35	147 - 313	100
	9.07	177 - 338	100
	12.97	217 - 367	100
	18.53	247 - 417	100
	26.39	298 - 472	100
	40.33	397 - 592	100
	1.97	27 - 273	100
	3.96	107 - 298	100
	5.79	136 - 298	100
	11.66	176 - 358	100
	24.35	296 - 477	100

et al. [9] and that of SF_6/N_2 and SF_6/CO_2 mixtures [26]. We observe a synergism in both C_4F_7N/N_2 and C_4F_7N/CO_2 mixtures, although the $(E/N)_{crit}$ of C_4F_7N/N_2 is higher than that of C_4F_7N/CO_2 mixtures. Mixtures of $\sim 13.5\%$ C_4F_7N in N_2 or $\sim 18.5\%$ C_4F_7N in CO_2 would have about the same $(E/N)_{crit}$ as pure SF_6, although as mentioned in section 2.3, the values for $(E/N)_{crit}$ presently obtained at low pressures may not apply at high pressure. The $(E/N)_{crit}$ we obtain for C_4F_7N/CO_2 mixtures differs by up to 15% from that found by Nechmi et al.

3. Discussion

3.1. Electron attachment to C_4F_7N

The effective ionization rate coefficient in C_4F_7N/N_2 and C_4F_7N/CO_2 mixtures shown in figures 1(a) and 2(a) decreases fast with decreasing E/N, which suggests that electron attachment to C_4F_7N is strongest at thermal electron energies. The present estimations of the attachment cross section might not yield the exact shape of the attachment cross section, due to the uncertainties in the EEDF of the carrier gases and the limited information content of the measurements. However, the present estimations suggest that the attachment cross section of C_4F_7N is similar to that of SF_6 for electron energies below

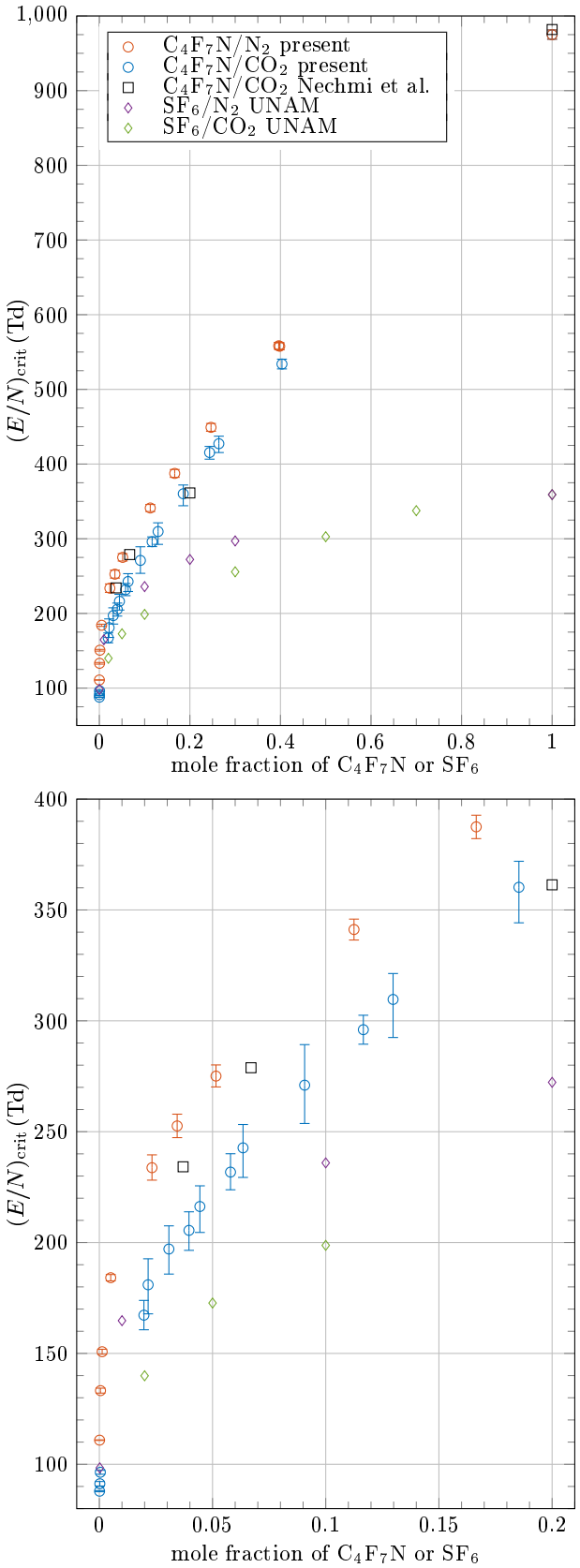

Figure 11. Density-reduced critical electric field of C_4F_7N/N_2, C_4F_7N/CO_2, SF_6/N_2 and SF_6/CO_2 mixtures.

0.1 eV, and that it is substantially larger than that of SF_6 in the region between 0.1 eV and 1 eV. The attachment around 1 eV could be due to dissociative attachment to CN^- similarly to other perfluorinated nitriles [27, 28], whereas electron attachment towards 0 eV could be parent ion attachment to $C_4F_7N^-$.

3.2. Ion kinetic processes in C_4F_7N

The complexity of the measured current in pure C_4F_7N at pressures > 100 Pa on the ionic time scale suggests that ion kinetics play a major role in C_4F_7N discharges at high pressures. From first modelling attempts, we suspect that at least two negative ion species are formed, which both exhibit electron detachment. Our present measurements at low pressures let us obtain the rate and transport coefficients of electrons. Based on these results we can attempt to model the ion kinetics in more detail in a future study.

3.3. Density-reduced critical electric field

The present results obtained at low pressures are insufficient to assess the performance of C_4F_7N as an electrical insulation gas, as the breakdown process at higher pressures might be affected by ion kinetics. We suspect this is why we obtain an $(E/N)_{\mathrm{crit}}$ of about 2.6 times that of SF_6, whereas the breakdown voltage of C_4F_7N is reported to be only 2 times that of SF_6 [1, 2].

The discrepancy in the density-reduced critical field of C_4F_7N/CO_2 mixtures from the present work compared to that of Nechmi et al. is likely due to a large uncertainty in the latter work. The authors give no uncertainty estimation, but the scatter in the data from figure 5 of their article suggests that a large uncertainty must be considered. In addition, the assumption made by the authors of a linearity in the logarithm of the measured current against the electrode spacing is not verified for electron attaching gases, as pointed out by Harrison and Geballe [29], and this could significantly affect their results.

Conclusion

We report electron rate and transport coefficients in pure C_4F_7N and in mixtures of C_4F_7N with N_2 and CO_2, and find that C_4F_7N has a large electron attachment cross section at thermal energies and up to 1 eV. Our measurements in C_4F_7N at pressures of a few hundred pascal show that ion kinetics are important in C_4F_7N discharges. The present results at low pressures enable us to obtain the rate and transport coefficients of electrons, which lays a solid basis for future modelling work, in which we will aim to obtain ion rate and transport coefficients in order to accurately model high pressure C_4F_7N discharges.

Acknowledgments

This work is financially supported by GE Grid (Switzerland) GmbH, Pfiffner Technologie AG, ABB Switzerland Ltd and Siemens AG. The sample of C_4F_7N was provided by GE Grid, Oberentfelden, Switzerland.

References

[1] Costello M, Flynn R and Bulinski M 2013 Fluorinated nitriles as dielectric gases WO Patent App. PCT/US2013/031,854 URL https://encrypted.google.com/patents/WO2013151741A1?cl=en

[2] Kieffel Y, Girodet A, Biquez F, Ponchon P, Owens J, Costello M, Bulinski M, San R V and Werner K 2014 SF_6 alternative development for high voltage switchgears *Cigre, Paris* paper D1-305 URL https://e-cigre.org/publication/SESSION2014-2014-cigre-session-set-of-papers--proceedings

[3] Laruelle E, Ficheux A, Kieffel Y and Waldron M 2017 *Cigre Science & Engineering* **7** 102–108 URL https://e-cigre.org/publication/CSE007-cse-007

[4] 3M^{TM} Novec^{TM} 4710 Insulating Gas, environmental, Health and Safety Summary, Issued: 6/17 URL http://multimedia.3m.com/mws/media/1418731O/12633-novec-insulating-gas-tech-bulletin-4710-a4-celum.pdf?fn=prodinfo_novec1230.pdf

[5] Sulbaek Andersen M P, Kyte M, Andersen S T, Nielsen C J and Nielsen O J 2017 *Environmental Science & Technology* **51** 1321–1329 (*Preprint* http://dx.doi.org/10.1021/acs.est.6b03758) URL http://dx.doi.org/10.1021/acs.est.6b03758

[6] Blàzquez S, Antiolo M, Nielsen O J, Albaladejo J and Jimnez E 2017 *Chemical Physics Letters* **687** 297 – 302 ISSN 0009-2614 URL http://www.sciencedirect.com/science/article/pii/S0009261417308862

[7] Kieffel Y, Biquez F and Ponchon P 2015 Alternative gas to SF_6 for use in high voltage switchgears: g^3 *Cired, Lyon* paper 0230

[8] Myhre G, Shindell D, Bréon F M, Collins W, Fuglestvedt J, Huang J, Koch D, Lamarque J F, Lee D, Mendoza B, Nakajima T, Robock A, Stephens G, Takemura T and Zhang H 2013 Anthropogenic and natural radiative forcing *Climate Change 2013: The Physical Science Basis. Contribution of Working Group I to the Fifth Assessment Report of the Intergovernmental Panel on Climate Change* ed Stocker T, Qin D, Plattner G K, Tignor M, Allen S, Boschung J, Nauels A, Xia Y, Bex V and Midgley P (Cambridge, United Kingdom and New York, NY, USA: Cambridge University Press) pp 659–740 ISBN 978-1-107-66182-0 URL www.climatechange2013.org

[9] Nechmi H E, Beroual A, Girodet A and Vinson P 2017 *IEEE Transactions on Dielectrics and Electrical Insulation* **24** 886–892 ISSN 1070-9878

[10] ETHZ database URL www.lxcat.net/ETHZ

[11] Dahl D A, Teich T H and Franck C M 2012 *Journal of Physics D: Applied Physics* **45** 485201 URL http://stacks.iop.org/0022-3727/45/i=48/a=485201

[12] Häfliger P and Franck C M 2018 *Review of Scientific Instruments* **89** 023114 (*Preprint* https://doi.org/10.1063/1.5002762) URL https://doi.org/10.1063/1.5002762

[13] Chachereau A, Rabie M and Franck C M 2016 *Plasma Sources Science and Technology* **25** 045005 URL http://stacks.iop.org/0963-0252/25/i=4/a=045005

[14] Chachereau A, Hösl A and Franck C M 2018 *J. Phys. D: Appl. Phys.* **51** 335204 URL http://dx.doi.org/10.1088/1361-6463/aad174

[15] Rabie M, Haefliger P, Chachereau A and Franck C M 2015 *Journal of Physics D: Applied Physics* **48** 075201 URL http://stacks.iop.org/0022-3727/48/i=7/a=075201

[16] Xiong J, Li X, Wu J, Guo X and Zhao H 2017 *Journal of Physics D: Applied Physics* **50** 445206 URL http://stacks.iop.org/0022-3727/50/i=44/a=445206

[17] Hagelaar G and Pitchford L 2005 *Plasma Sources Science and Technology* **14** 722–733 ISSN 0963-0252 URL http://dx.doi.org/10.1088/0963-0252/14/4/011

[18] Biagi database, data extracted from the fortran program MAGBOLTZ of S.F. Biagi, versions 8.9 and after, data retrieved on April 19, 2017 URL www.lxcat.net/Biagi

[19] Phelps database data retrieved on June 27, 2014 URL www.lxcat.net/Phelps

[20] Braun M, Marienfeld S, Ruf M W and Hotop H 2009 *Journal of Physics B: Atomic, Molecular and Optical Physics* **42** 125202 URL http://stacks.iop.org/0953-4075/42/i=12/a=125202

[21] Verhaart H F A and van der Laan P C T 1984 *Journal of Applied Physics* **55** 3286–3292 URL https://doi.org/10.1063/1.333364

[22] Hösl A, Häfliger P and Franck C M 2017 *Journal of Physics D: Applied Physics* **50** 485207 URL http://stacks.iop.org/0022-3727/50/i=48/a=485207

[23] Haefliger P, Hösl A and Franck C M 2018 *Journal of Physics D: Applied Physics* **51** 355201 URL http://stacks.iop.org/0022-3727/51/i=35/a=355201

[24] Pancheshnyi S 2013 *Journal of Physics D: Applied Physics* **46** 155201 URL http://stacks.iop.org/0022-3727/46/i=15/a=155201

[25] Wang W and Bogaerts A 2016 *Plasma Sources Science and Technology* **25** 055025 URL http://stacks.iop.org/0963-0252/25/i=5/a=055025

[26] UNAM database data retrieved on January 27, 2017 URL www.lxcat.net/UNAM

[27] Wooton R E 1982 Gases superior to SF_6 for insulation and interruption *EPRI EL-2620, Final Report*

[28] Heni M, Illenberger E and Lentz D 1986 *International Journal of Mass Spectrometry and Ion Processes* **71** 199 – 210 ISSN 0168-1176 URL http://www.sciencedirect.com/science/article/pii/016811768685056X

[29] Harrison M A and Geballe R 1953 *Phys. Rev.* **91**(1) 1–7 URL https://link.aps.org/doi/10.1103/PhysRev.91.1